Research Article

Journal of Physical Organic Chemistry

Received: 1 April 2008, Revised: 10 July 2008, Accepted: 1 August 2008, Published online in Wiley InterScience: 17 September 2008

(www.interscience.wiley.com) DOI 10.1002/poc.1439

Kinetics and mechanism for acid-catalyzed disproportionation of 2,2,6,6-tetramethylpiperidine-1-oxyl

Vasily D. Sen'[a]* and Valery A. Golubev[a]

Disproportionation of cyclic nitroxyl radicals (NRs) in acid solutions is of key importance for the chemistry of these compounds. Meanwhile, the data reported on the mechanism of this reaction in dilute acids are inconsistent with those on the stability of NRs in concentrated acids. Here we have examined the kinetics and stoichiometry for the disproportionation of 2,2,6,6-tetramethylpiperidine-1-oxyl (1) in aqueous H_2SO_4 (1.0–99.3 wt%) and found that (1) the disproportionation of 1 proceeds by the same mechanism over the entire range of acid concentrations, (2) the effective rate constant of the process exhibits a bell-shaped dependence on the excess acidity function *X* peaked at $X = -pK_{1H+} = 5.8 \pm 0.3$, (3) a key step of the process involves the oxidation of 1 with its protonated counterpart $1H^+$ yielding oxopiperidinium cation 2 and hydroxypiperidine 3 at a rate constant of $(1.4 \pm 0.8) \times 10^5\ M^{-1} \cdot s^{-1}$, and (4) the reaction is reversible and, upon neutralization of acid, disproportionation products 2 and $3H^+$ comproportionate to starting 1. In highly acidic media, the protonated form $1H^+$ is relatively stable due to a low disproportionation rate. Based on the known and newly obtained values of equilibrium constants, both the standard redox potential for the $1H^+/3$ pair (955 ± 15 mV) and the pH-dependences have been calculated for the reduction potentials of 1 and 2 to hydroxylamine 3 that is in equilibrium with its protonated $3H^+$ and deprotonated 3^- forms. The data obtained provide a deeper insight into the mechanism of nitroxyl-involving reactions in chemical and biological systems.

Supporting information may be found in the online version of this article.

Keywords: kinetics; mechanism; nitroxyl radicals; TEMPO; 2,2,6,6-tetramethylpiperidine-1-oxyl; protonation; electron transfer; reduction potentials; acidity function

INTRODUCTION

Cyclic nitroxyl radicals (NRs) are being widely used as EPR probes in chemical and biological studies.[1–3] Over the past two decades, ever increasing attention has been given to applications based on the capability of NRs and their redox counterparts to undergo rapid one- or two-electron transfer, as shown in Scheme 1 for the most popular their representative, 2,2,6,6-tetramethylpiperidine-1-oxyl (**1**).

The redox pair oxoammonium cation (**2**)/NR (**1**) is able to catalyze the dismutation of superoxide radical in a way similar to that in case of natural superoxide dismutase (SOD). Initially, NR reduces the protonated form of superoxide (i.e., hydroperoxide radical $HO_2^{\bullet}$) to give oxoammonium cation **2** and hydrogen peroxide. This is followed by oxidation of another superoxide radical $O_2^{\bullet-}$ with cation **2** leading to regeneration of **1** and formation of dioxygen (Scheme 2).[4,5]

In combination with cell permeability, such a property of NRs opens perspectives for their clinical application as drugs for treating diseases accompanied by oxidative stress.[6]

Another application of NRs is selective oxidation of alcohols with cation **2** to carbonyl or carboxyl compounds which takes place as a two-electron transfer process. This reaction is transformed into catalytic one when hydroxylamine **3** is reoxidized back to cation **2** with an appropriate primary oxidant which alone is ineffective for alcohols.[7–10] Any of compounds **1**–**3** can be used as a primary catalyst.

Due to facile charge transfer in the **2**/**1** redox pair and its stability, piperidine NRs may also be used as redox shuttle molecules for overcharge protection of Li-ion cells or even as cathode-active material in an organic-based battery.[11,12]

The redox cycle **1**–**2**–**3** (Scheme 1) involves the acid-independent **2**/**1** pair and acid-dependent **1**/**3** and **2**/**3** pairs. Under the action of strong acids (HA), NRs undergo disproportionation reaction involving two of this redox pairs, **2**/**1** and **1**/**3**. Besides piperidine nitroxyls[13,14] (see Scheme 3), the acid-induced disproportionation was observed for di-*tert*-butylnitroxyl,[15] nitronyl-,[16] and imidazoline-[17] NRs.

Deep insight into the mechanism and quantitative characterization of disproportionation reaction seem important for further promotion of the above-mentioned and new applications of NRs. For instance, the disproportionation reaction may turn out useful

* *Correspondence to: V. D. Sen', Institute of Problems of Chemical Physics, Russian Academy of Sciences, Chernogolovka, Moscow Region 142432, Russia. E-mail: senvd@icp.ac.ru*

a *V. D. Sen', V. A. Golubev*
Institute of Problems of Chemical Physics, Russian Academy of Sciences, Chernogolovka, Moscow Region 142432, Russia

Journal of Physical Organic Chemistry

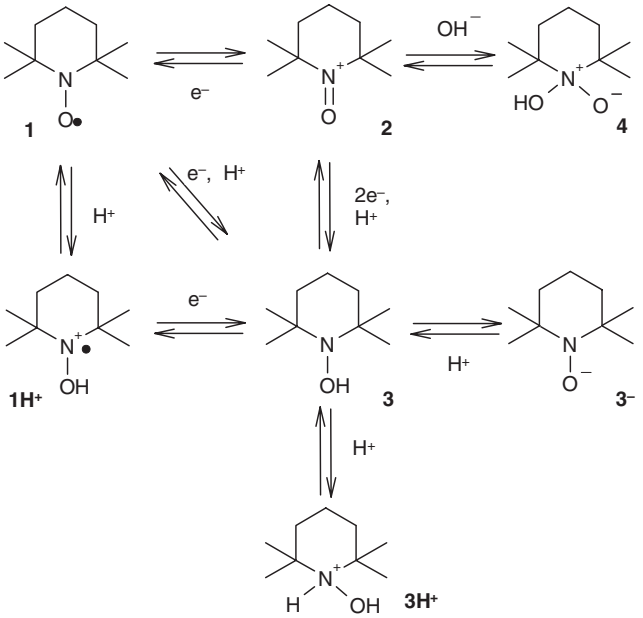

Scheme 1. Redox cycle **1**–**2**–**3** and related acid–base equilibria for NR **1**

for identification of reactive sites in heteropolyacids.[18] Another interesting example is the rapid and reversible disproportionation of NRs covalently bonded in the major groove of DNA.[19] In this case, the easiness of disproportionation and regeneration of NRs upon variation in pH can be indicative of either favorable for electron transfer arrangement of NRs linked with DNA or of the occurrence of electron transfer through the DNA chain. In order to shed light on the mechanism of the NRs-catalyzed oxidation of alcohols, the acid-catalyzed disproportionation of **1** in a nonaqueous solution has been studied by electrochemical methods.[20]

Previously, we studied the kinetics of disproportionation reaction for **1** within a limited range of acid concentration (≤0.2 M), which did not allow us to quantitatively characterize all steps of the proposed reaction mechanism.[21] Meanwhile, the kinetics of this reaction in concentrated acids has not been explored so far. The absence of EPR signal from radical **1** dissolved in concentrated (40–80%; here and hereinafter, wt%) aqueous H_2SO_4 was associated[22] with line broadening due to rapid proton exchange between **1** and its protonated counterpart $\mathbf{1H}^+$ (Scheme 1). Inconsistency between the data of[13,14,21] and[22] was briefly discussed by Volodarsky *et al.*[23]

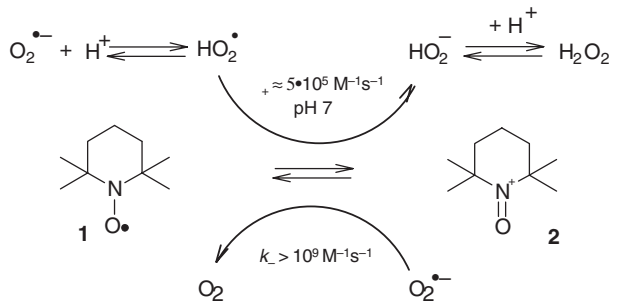

Scheme 2. SOD-mimetic activity of NRs

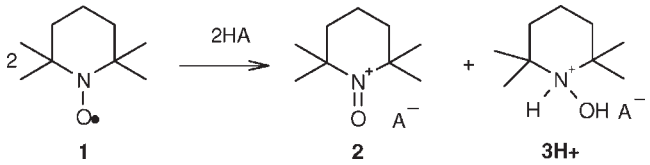

Scheme 3. Disproportionation of radical **1** under the action of strong acids

For further insight into the mechanism of disproportionation reaction, we studied its kinetics for radical **1** within a wide range of acid concentrations in terms of the excess acidity concept and found that acid-catalyzed disproportionation of NRs in both dilute and concentrated acids proceeds by the same mechanism. The rate and/or equilibrium constants for all steps of disproportionation reaction for **1** have been calculated based on the obtained and literature data. The known value of $E^0_{\mathbf{2/1}}$ and obtained equilibrium constants were also used to determine the standard reduction potential for the $\mathbf{1H}^+/\mathbf{3}$ pair and the pH-dependences have been calculated for the reduction potentials of **1** and **2** to hydroxylamine **3** that is in equilibrium with its protonated $\mathbf{3H}^+$ and deprotonated $\mathbf{3}^-$ forms ($E_{\mathbf{1/3}\Sigma}$ and $E_{\mathbf{2/3}\Sigma}$, respectively).

EXPERIMENTAL

Kinetics

The kinetics of disproportionation of **1** in H_2SO_4 was studied by EPR or absorption spectroscopy. EPR spectra were taken (at 25 ± 1 °C) with an EPA-2M spectrometer using glass ampoules about 1 mm in their inner diameter. At $[\mathbf{1}] \leq 5 \times 10^{-4}$ M, the intensity of EPR signal from **1** was found to be a linear function of [**1**]. Changes in the *Q*-factor of a resonator were taken into account upon gluing a thin cell with the reference sample of solid 2,2-diphenyl-1-picrylhydrazyl (DPPH) to a working ampoule. Reaction mixtures were prepared either by adding solid **1** (purified by vacuum sublimation) to aqueous H_2SO_4 (analytical grade) at ~20 °C under intense stirring or by mixing a small portion of a 0.1–0.01 M aqueous solution of **1** with an ice-cooled solution of H_2SO_4. The reaction rates were determined from the consumption of **1** in 1.0–27.1% H_2SO_4 or from the consumption of $\mathbf{1H}^+$ in 86.4–99.3% H_2SO_4. At $[H_2SO_4]$ = 30–85%, the reaction rate was too high to be measured by conventional technique. The concentration of **1** was calculated from the expression: $[\mathbf{1}] = (I I^0_{st}/I^0 I_{st})[1]_0$, where I, I_0, I_{st}, and I^0_{st} refer to the amplitudes of EPR signals from the reaction mixture, from the aqueous reference solution of **1** of a known concentration, and from the DPPH sample when the working ampoule was filled with either H_2SO_4 solution or water, respectively; and $[\mathbf{1}]_0$ is the concentration of **1** in the aqueous reference solution. The I^0_{st}/I_{st} ratio depends on $[H_2SO_4]$ and can attain a value up to 1.5.

The EPR spectrum of $\mathbf{1H}^+$ in concentrated H_2SO_4 consists of three doublets[22] with close linewidths, which is typical of the triplet EPR signal from **1** in water (Fig. 1).

In view of identical linewidths and different multiplicity of the **1** and $\mathbf{1H}^+$ spectra, the concentration of cation radical $\mathbf{1H}^+$ was calculated from the expression: $[\mathbf{1H}^+] = [(I_1 + I_2) I^0_{st}/I^0 I_{st}][1]_0$, where $I_1 + I_2$ is a sum of the amplitudes of two components of the low-field doublet in the spectrum of $\mathbf{1H}^+$ (Fig. 1). In concentrated H_2SO_4, the initial $[\mathbf{1H}^+]$ does not exceed 3% of the value corresponding to the added amount of **1**, presumably, due

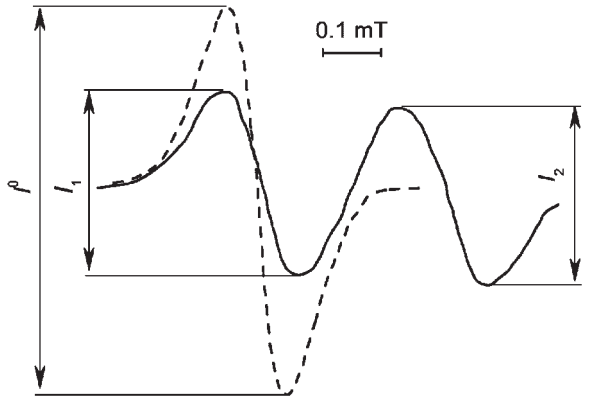

Figure 1. Low-field EPR-signal from **1** in water (dashed) and low-field doublet of $\mathbf{1H}^+$ in 99.3% H_2SO_4 (solid line)

to relatively slow (~2 min) dissolution of **1** and its rapid disproportionation to **2** and $\mathbf{3H}^+$ on the surface of crystals. This is also supported by somewhat higher initial $[\mathbf{1H}^+]_0$ upon dissolution of fine crystals of **1**. The value of $[\mathbf{1H}^+]$ as determined from the first record of the EPR spectrum of the reaction solution was regarded as the initial $[\mathbf{1H}^+]_0$ ($t = 0$).

Absorption spectra were taken with a Specord UV–Vis spectrophotometer. The absorption spectrum of **1** in water exhibits two bands peaked at λ_{max} 428 ($\varepsilon = 12.5 \pm 0.2$) and 245 nm ($\varepsilon = 1970 \pm 50\ M^{-1} \cdot cm^{-1}$).[21] For $[\mathbf{2}] \leq 10^{-2}$ M, the absorption spectra of **2** are independent of the type of anion ($A^- = Cl^-$ or $0.5SO_4^{2-}$) present in solution and show two bands with maxima at λ_{max} 470 ($\varepsilon = 19.5 \pm 0.2$) and 236 nm ($\varepsilon = 1770 \pm 50\ M^{-1} \cdot cm^{-1}$)[21] (see Supplementary Material, Fig. S1). The reaction rates were determined from the consumption of radical **1** and accumulation of cation **2** using the following relationships:

$$[\mathbf{1}] = [D_1(\varepsilon_{\mathbf{2}})_2 - D_2(\varepsilon_{\mathbf{2}})_1]/10[(\varepsilon_{\mathbf{1}})_1(\varepsilon_{\mathbf{2}})_2 - (\varepsilon_{\mathbf{2}})_1(\varepsilon_{\mathbf{1}})_2]$$

$$[\mathbf{2}] = [D_1(\varepsilon_{\mathbf{1}})_2 - D_2(\varepsilon_{\mathbf{1}})_1]/10[(\varepsilon_{\mathbf{2}})_1(\varepsilon_{\mathbf{1}})_2 - (\varepsilon_{\mathbf{1}})_1(\varepsilon_{\mathbf{2}})_2]$$

where D is the optical density of reaction mixture in a 10-cm cell and ε are the molar extinction coefficients of **1** ($\varepsilon_{\mathbf{1}}$) and **2** ($\varepsilon_{\mathbf{2}}$) in water: $(\varepsilon_{\mathbf{1}})_1 = 9.4 \pm 0.1$, $(\varepsilon_{\mathbf{1}})_2 = 5.8 \pm 0.1$, $(\varepsilon_{\mathbf{2}})_1 = 5.2 \pm 0.1$, and $(\varepsilon_{\mathbf{2}})_2 = 19.5 \pm 0.2\ M^{-1} \cdot cm^{-1}$. The outer subscripts 1 and 2 pertain to the wavelengths 397 and 481 nm, respectively. In this spectral range, the solutions of **3** were transparent. Errors in kinetic calculations are given in terms of standard deviations.

Stoichiometry

The above spectrophotometric determination of **1** and **2** affords also to control the reaction stoichiometry. At 100% selectivity of the disproportionation reaction, the condition $[\mathbf{1}]_0 = [\mathbf{1}] + 2[\mathbf{2}]$ should hold true (see Scheme 3), where $[\mathbf{1}]_0$ is the initial and $[\mathbf{1}]$ and $[\mathbf{2}]$ are the running concentrations of **1** and **2**. The fulfillment of this condition in dilute H_2SO_4 is supported by the data in Fig. S2 (see Supplementary Material). Checking its validity in concentrated H_2SO_4 was made as follows. A solution of NR **1** (2×10^{-2} M, 2 ml) was added to 2 ml of 93% H_2SO_4 within 5 min under stirring and ice cooling. The absorption spectrum of the obtained solution in ~58% H_2SO_4 in the visible was nearly the same as the spectrum of 5×10^{-3} M solution of salt **2** ($A^- = ClO_4^-$, synthesized as described in Ref.14) in 58% H_2SO_4. This means that, in concentrated H_2SO_4, the disproportionation of 1 mol **1** also gives rise to selective formation of 0.5 mol of salts **2** and $\mathbf{3H}^+$. The reaction mixture was EPR-silent before and after its dilution with water to a total volume of 40 ml. To this dilute solution, solid $NaHCO_3$ (7.5 g) was added in small portions under stirring and ice cooling until pH 7–8, and the mixture was allowed to stay at ~25 °C for 1 h. In doing so, the comproportionation reaction between **2** and **3** took place with 96 ± 3% regeneration of **1** as evidenced by EPR measurements. Therefore, the disproportionation of **1** features high selectivity and reversibility over the entire acidity range.

RESULTS AND DISCUSSION

Kinetic study

According to our data and Ref.22 the EPR spectrum of **1** in solution, for $[H_2SO_4] \leq 30\%$, consists of three lines ($a_N = 1.73$ mT) attributed to unprotonated **1**; while for $[H_2SO_4] \geq 85\%$ it exhibits three doublets ($a_N = 2.15$ mT, $a_H = 0.31$ mT) assigned to cation radical $\mathbf{1H}^+$. At intermediate $[H_2SO_4]$, as-prepared solutions of **1** are EPR-silent. To account for such facts as these, the authors[22] set up the hypothesis of broadening the EPR-signal due to fast proton exchange between **1** and $\mathbf{1H}^+$ at $30\% \leq [H_2SO_4] \leq 85\%$. But our previous[21] and newly obtained results presented below are in contradiction with this assumption.

Radical **1** at $[H_2SO_4] \leq 30\%$ and cation radical $\mathbf{1H}^+$ at $[H_2SO_4] \geq 85\%$ decay at a rate which depends on acid concentration. Both the processes, consumption of **1** and $\mathbf{1H}^+$, obey the second-order kinetics (with respect to $[\mathbf{1}]$ and $[\mathbf{1H}^+]$, respectively) over a wide range $[(2–50) \times 10^{-5}\ M]$ of initial concentrations C_0. With increasing $[H_2SO_4]$, the effective rate constants k_{ef} were found to grow in the range of 1–27.1% and drop in the range of 86.4–99.3% (see Supplementary Material). The effective rate constants k_{ef} as derived from optical absorption spectra at $[\mathbf{1}]_0 = (3–10) \times 10^{-3}$ M and $[H_2SO_4] = 1.0–10.2\%$ coincide with those determined from EPR data. In a course of reaction, the sum $[\mathbf{1}] + 2[\mathbf{2}]$ as derived from optical measurements remains virtually unchanged and equal to $[\mathbf{1}]_0$. The data on preparative yields of **2** and $\mathbf{3H}^+$ ($A^- = 0.5SO_4^{2-}$) obtained in reaction of **1** with concentrated H_2SO_4[14] well agree with the stoichiometry depicted in Scheme 3. Taken together, these data clearly indicate that, on going from dilute to concentrated acids, the mechanism of disproportionation of **1** remains to be the same and includes reactions (1–3). Stoichiometric Eqn (4) is the sum of reactions (1–3).

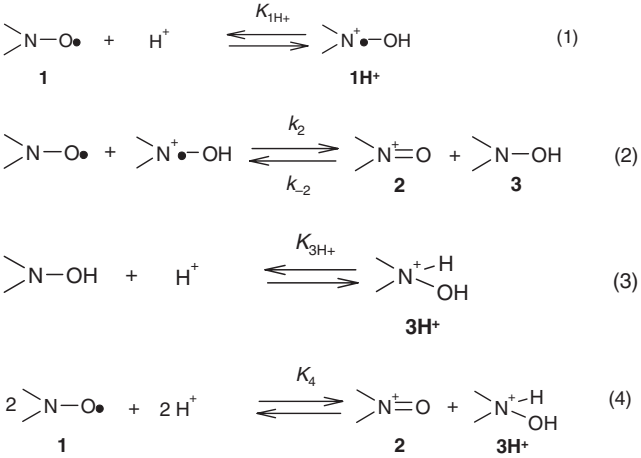

For pH ≤ 2, equilibrium (4) shifts to the right[21] and, hence, the rate of the reverse comproportionation reaction between **2** and **3** is negligibly small for $[H_2SO_4] = 1.0$–99.3%. Preliminary analysis of the kinetic data by the use of Hammett's acidity function H_0 has shown that, in the range $[H_2SO_4] = 1.0$–27.1%, the slope of the $\log k_{ef}$–H_0 plot is equal to 1.35. For analysis of acid-catalyzed reactions for which $\Delta(\log k_{ef})/\Delta H_0 \neq 1$, most convenient seems to be the excess acidity function approach.[24]

According to the proposed mechanism and in terms of the Cox and Yates approach,[24] the disproportionation rate for **1** can be written in the form:

$$-d([\mathbf{1}] + [\mathbf{1H}^+])/dt = k_{ef}[\mathbf{1}]_\Sigma^2 = 2k_2^0 a_{\mathbf{1}} a_{\mathbf{1H}+}/f_{\neq} =$$
$$= 2k_2^0[\mathbf{1}][\mathbf{1H}^+](f_{\mathbf{1}} f_{\mathbf{1H}+}/f_{\neq}) \quad (5)$$

Here k_{ef} is the measured rate constant; k_2^0 the medium-independent rate constant[25] of reaction (2) (in dilute solution); [**1**], [**1H**$^+$], and $[\mathbf{1}]_\Sigma$ the concentrations of **1**, **1H**$^+$ and their sum, respectively; *a* and *f* the activities and activity coefficients of the reagents; $f_{\neq}$ the activity coefficient of the transition state.

Given that $[\mathbf{1}]_\Sigma = [\mathbf{1}] + [\mathbf{1H}^+]$ and $K_{\mathbf{1H}+} = ([\mathbf{1}][H^+]/[\mathbf{1H}^+])(f_{\mathbf{1}} f_{H+}/f_{\mathbf{1H}+})$, after necessary transformations (see Supplementary Material) we come to Eqns (6) and (7) describing the dependence of k_{ef} on the excess acidity function *X* for $[H_2SO_4] \leq 30\%$ (Eqn 6) and $[H_2SO_4] \geq 85\%$ (Eqn 7), respectively.

$$\log k_{ef} - \log [H^+] = \log(2k_2^0) + pK_{\mathbf{1H}+} + m^{\#}m^*X + \log f_{\mathbf{1}} \quad (6)$$

$$\log k_{ef} + \log [H^+] = \log(2k_2^0) - pK_{\mathbf{1H}+} + (m^{\#} - 2)m^*X + \log f_{\mathbf{1}} \quad (7)$$

Here m^* and $m^{\neq}$ are the slope parameters[24] typical of equilibrium (1) and the transition state in the rate-limiting step (2), respectively. For $[H_2SO_4] = 1.0$–27.1%, the plot of $\log k_{ef} - \log [H^+]$ *versus X* was found to be linear (Fig. 2, line *1*), with a slope equal to 1.95 ± 0.09, intercept of -0.47 ± 0.04, and correlation coefficient of 0.993.

For $[H_2SO_4] = 86.4$–99.3%, the plot of $\log k_{ef} + \log [H^+]$ *versus X* was also found to be linear (Fig. 2, line *2*), with a slope of -1.16 ± 0.06, intercept of 11.20 ± 0.54, and correlation coefficient of 0.996.

At $X = 0$, the intercepts of plots *1* and *2* are equal to $\log(2k_2^0) + pK_{\mathbf{1H}+} + \log f_{\mathbf{1}}$ and $\log(2k_2^0) - pK_{\mathbf{1H}+} + \log f_{\mathbf{1}}$, respectively. From the difference and sum of these expressions (at the evident condition $\log(2k_2^0) \gg \log f_{\mathbf{1}}$), we obtain: $pK_{\mathbf{1H}+} = -5.8 \pm 0.3$, $K_{\mathbf{1H}+} = (8 \pm 4) \times 10^5$ M, and $k_2^0 = (1.4 \pm 0.8) \times 10^5$ M$^{-1} \cdot$ s^{-1}. Large uncertainty in the values of $K_{\mathbf{1H}+}$ and k_2^0 arise largely from the long-range extrapolation of line *2* to $X = 0$ (Fig. 2). A good agreement between the ratios of mean values – $k_2^0/K_{\mathbf{1H}+} = 1.4 \times 10^5/8 \times 10^5 = 0.18$ M$^{-2} \cdot$ s^{-1} for concentrated H_2SO_4 and $k_2/K_{\mathbf{1H}+} = 0.21$ M$^{-2} \cdot$ s^{-1} for dilute ($\leq$0.2 M) acids[21] – can be regarded as an evidence for the applicability of our approach.

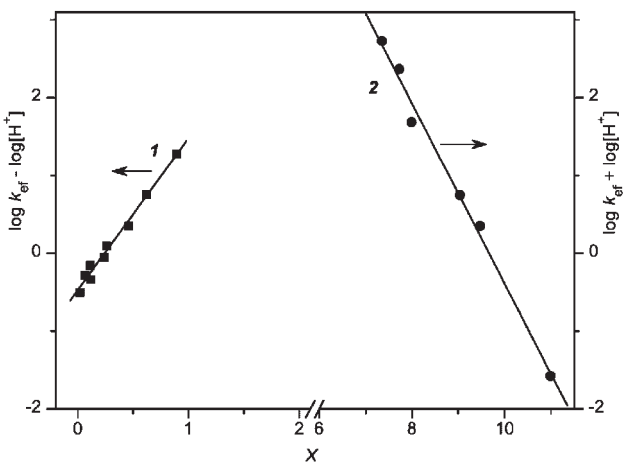

Figure 2. Excess acidity analysis of the disproportionation of **1** in sulfuric acid at 25 °C: (*1*) $\log k_{ef} - \log [H^+]$ *versus X* and (*2*) $\log k_{ef} + \log [H^+]$ *versus X*

The above data show that $\log k_{ef}$ exhibits a bell-shaped dependence on *X*; maximum value of k_{ef} correspond to such value of *X* at which $a_{\mathbf{1}} = a_{\mathbf{1H}+}$. The measured values of $\log k_{ef}$ lie on the linear wings of this dependence. From the slopes of plots *1* and *2* in Fig. 2 – $m^{\neq}m^* = 1.95 \pm 0.09$ and $(m^{\neq} - 2)m^* = -1.16 \pm 0.06$, respectively – we obtain: $m^{\neq} = 1.25 \pm 0.05$ and $m^* = 1.56 \pm 0.14$. Similar values of parameter m^* are typical of tertiary anilines and indoles.[26] The rate and equilibrium constants defining the disproportionation of **1** in aqueous acids are summarized in Table 1.

Reduction potentials

The data of Table 1 and the reported[27] value of $E^0_{\mathbf{2/1}} = 750 \pm 5$ mV (reported data on the half-wave potential are $E_{\mathbf{2/1}} = 740 \pm 10$[28] and 732 mV[29]) were used to calculate the standard reduction potential $E^0_{\mathbf{1H+/3}}$ and the pH-dependence of the reduction potential of **1** to the sum of **3H**$^+$, **3**, and **3**$^-$. The reduction of **1** to the sum of **3H**$^+$, **3**, and **3**$^-$ includes half-reaction (8) and acid–base equilibria (3) and (9).

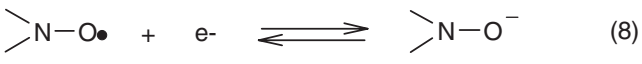

1 **3**$^-$ (8)

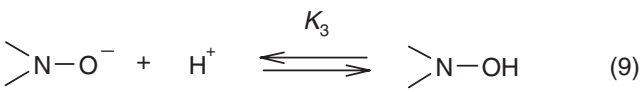

3$^-$ **3** (9)

Given that $[\mathbf{3}]_\Sigma = [\mathbf{3H}^+] + [\mathbf{3}] + [\mathbf{3}^-] = [\mathbf{1}]$, the dependence of $E_{\mathbf{1/3}\Sigma}$ on a_{H+} can be written in the form[28]:

$$E_{\mathbf{1/3}\Sigma} = E^0_{1/3-} - (RT/F)\ln K_3 K_{\mathbf{3H}+}$$
$$+ (RT/F)\ln(K_3 K_{\mathbf{3H}+} + a_{H+}K_{\mathbf{3H}+} + a_{H+}^2) \quad (10)$$

Table 1. Rate and equilibrium constants for disproportionation of **1** in aqueous acids at 25 °C

Constant	Value	Ref.
$pK_{\mathbf{1H}+}$	-5.8 ± 0.3	This work
	-5.5 ± 1	22
k_2^0 (M$^{-1} \cdot$ s^{-1})	$(1.4 \pm 0.8) \times 10^5$	This work
k_{-2} (M$^{-1} \cdot$ s^{-1})	51 ± 1	21
	52 ± 1	28
$pK_{\mathbf{3H}+}$	6.90 ± 0.02	21
	7.5	28
K_4 (M^{-2})	$(3.3 \pm 0.2) \times 10^4$	21

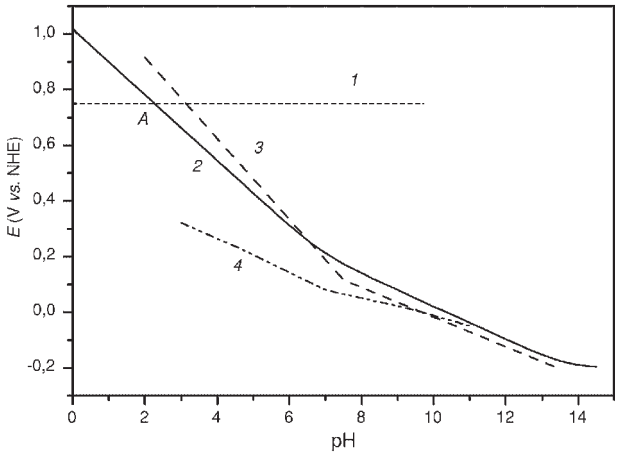

Figure 3. Reduction potential $E^0_{2/1}$ (*1*) and $E_{1/3\Sigma}$–pH relationships as calculated from Eqn (10) (*2*) and obtained by voltammetric[28] (*3*) and polarographic[31] (*4*) measurements

Taking the value of $K_4 = ([\mathbf{2}][\mathbf{3}]_\Sigma)/([\mathbf{1}]^2 a^2_{H+}) = 3.3 \times 10^4\ M^{-2}$ from Table 1, we obtain that, at pH 2.26 $([\mathbf{2}][\mathbf{3}]_\Sigma)/[\mathbf{1}]^2 = 1$. At this pH value (point *A* in Fig. 3), the potentials of both direct and reverse reactions are identical and equal to $E_{1/3\Sigma} = E^0_{2/1} = 750$ mV. At pH 0, the last term in Eqn (10) is negligible, whence it follows that $E_{1/3\Sigma} = E^0_{1/3-} - (RT/F)\ln K_3 K_{3H+} = E^0_{2/1} + (RT/F)\ln K_4 = 1017$ mV. Assuming that $K_3 = 2 \times 10^{-14}$ M (just as for H_2NOH[30]), from Eqn (10) we can estimate the value of $E^0_{1/3-} = -213$ mV. At pH ≤ 12, the value of K_3 has no influence on the $E_{1/3\Sigma}$–pH plot of Eqn (10) (Fig. 3, curve *2*).

With account of uncertainty in the constants used, the error bar for curve *2* in the range pH ≤ 12 must not exceed ± 10 mV. Curve *2* calculated from equilibrium constants and the voltammetrically determined curve *3* well agree, except for the range of low pH where the voltammetric data[28] presumably may have a systematic error. As follows from Scheme 1, the two-electron reduction potential $E_{2/3\Sigma} = E^0_{2/1} + E_{1/3\Sigma}$. Note that, at pH ≥ 11, cation **2** is known[29,32] to add OH^-, thus forming N-oxide **4** (Scheme 1). Therefore, in alkaline media its reduction potential can be expected to decrease. The value of $pK_{3H+} = 6.90 \pm 0.02$ measured[21] with a thoroughly calibrated pH meter is markedly lower than the value of 7.5 estimated[28] from the inflexion point in the $E_{1/3\Sigma}$–pH plot (see Supplementary Material).

For cation radical $\mathbf{1H}^+$, its standard reduction potential was calculated from the equation $E^0_{1H+/3} = E^0_{2/1} + (RT/F)\ln K_2$. Taking $K_2/K_{1H+} = (4.1 \pm 0.3) \times 10^{-3}\ M^{-1}$ (from Ref. 21) and $K_{1H+} = (8 \pm 4) \times 10^5$ M, we obtain that $E^0_{1H+/3} = 955 \pm 15$ mV. For the simplest cation radical $H_2N^{\bullet+}$—OH, estimates[33] gave that its E^0 value is 1.3 ± 0.1 V, which is markedly higher than the value of $E^0_{1H+/3}$, which can associated, at least in part, with the + *I*-effect of alkyl substituents in $\mathbf{1H}^+$.

Stability of NRs toward acid disproportionation

The equilibrium constant $K_4 = K_2/K_{1H+}K_{3H+}$ is a measure of NRs resistance to their reversible acid-catalyzed disproportionation. NRs with electron withdrawing substituents exhibit higher values of K_{1H+} and K_{3H+}, lower value of K_4, and hence they are more resistant to disproportionation in acids.[21,23] For instance, imidazoline and nitronyl NRs are more acid-resistant than radical

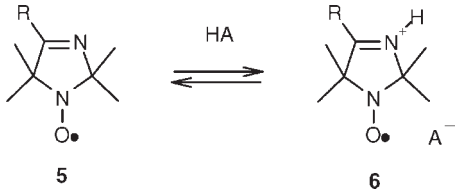

Scheme 4. Protonation of second basic group in imidazolinoxyls **5**

1 due to the –*I*-effect of the imino and nitrone groups, respectively. Moreover, in strong acids these groups undergo protonation, as shown in Scheme 4 for imidazolinoxyls **5**. In some cases, cation-radical salts **6** are stable enough to be isolated as analytically pure compounds.[23,34]

The basicity of the nitroxyl group in **6** further decreases in comparison to **5** due to protonation of imino group. For example, the half time of disproportionation $t_{1/2}$ in 36% HCl calculated for **1** by Eqn (5) and experimentally found for **5** (R = Ph)[35] at initial concentrations 5×10^{-4} M are equal to <1 s и ~ 12 min, respectively. Supposing that the value of k_2^0 only slightly depends on the type of NR, one may conclude that stability of NRs in acid media is defined mainly by the basicity of nitroxyl group. In contrast to piperidine-1-oxyl **1**, the disproportionation products of radical **5** are unstable and completely hydrolyze during ~48 h (36% HCl, 20 °C)[35] with disclosure of the imidazoline cycle.

CONCLUSIONS

(1) For the first time, all steps of the acid-catalyzed reversible disproportionation of NRs have been quantitatively characterized using radical **1** as an example.
(2) NRs are very weak bases. Piperidine-1-oxyl **1** is characterized by the value of $pK_{1H+} = -5.8 \pm 0.3$ which corresponds to half-protonation in ~64% H_2SO_4.
(3) Due to high reduction potential of protonated piperidine-1-oxyl $\mathbf{1H}^+$ ($E^0_{1H+/3} = 955 \pm 15$ mV), it is capable of oxidizing its unprotonated counterpart **1** to oxoammonium cation **2** ($E^0_{2/1} = 750 \pm 5$ mV) at the rate constant $k_2^0 = (1.4 \pm 0.8) \times 10^5\ M^{-1} \cdot s^{-1}$.
(4) Nitroxyls bearing electron-withdrawing substituents show a lower basicity of their nitroxyl group and a higher stability in acidic media. The degree of reversibility of the acid-catalyzed disproportionation for particular NRs may be used as a measure of stability of their "NR–oxoammonium cation–hydroxylamine" redox cycle.

REFERENCES

[1] L. B. Volodarsky (Ed.), *Imidazoline Nitroxides*, Vol. 2. CRC Press, Boca Raton, **1988**.
[2] R. I. Zhdanov (Ed.), *Bioactive Spin Labels*, Springer, Berlin, **1992**.
[3] L. J. Berliner (Ed.), *Spin Labeling: The Next Millennium*, Plenum Press, New York, **1998**.
[4] V. D. Sen', V. A. Golubev, I. V. Kulyk, E. G. Rozantsev, *Russ. Chem. Bull.* **1976**, *25*, 1647–1654.
[5] S. Goldstein, G. Merenyi, V. Russo, A. Samuni, *J. Am. Chem. Soc.* **2003**, *125*, 789–795.
[6] B. P. Soule, F. Hyodo, K. Matsumoto, N. L. Simone, J. A. Cook, M. C. Krishna, J. B. Mitchell, *Free Rad. Biol. Med.* **2007**, *42*, 1632–1650.
[7] V. A. Golubev, Y. N. Kozlov, A. N. Petrov, A. P. Purmal, *Prog. React. Kinet.* **1991**, *16*, 35–54.

[8] A. E. J. de Nooy, A. S. Besemer, H. van Bekkum, *Synthesis* **1996**, 1153–1174.
[9] R. A. Sheldon, I. W. C. E. Arends, *Adv. Synth. Catal.* **2004**, *346*, 1051–1071.
[10] N. Merbouh, J. M. Bobbitt, C. Brückner, *Org. Prep. Proc. Int.* **2004**, *36*, 1–31.
[11] L. M. Moshurchak, C. Buhrmester, R. L. Wang, J. R. Dahn, *Electrochim. Acta* **2007**, *52*, 3779–3784.
[12] T. Suga, H. Konishi, H. Nishide, *Chem. Commun.* **2007**, 1730–1732.
[13] V. A. Golubev, E. G. Rozantsev, M. B. Neiman, *Russ. Chem. Bull.* **1965**, *14*, 1898–1904.
[14] V. A. Golubev, R. I. Zhdanov, V. M. Gida, E. G. Rozantsev, *Russ. Chem. Bull.* **1971**, *20*, 768–770.
[15] A. K. Hoffman, A. T. Henderson, *J. Am. Chem. Soc.* **1961**, *83*, 4671–4672.
[16] J. H. Osiecki, E. F. Ullman, *J. Am. Chem. Soc.* **1968**, *90*, 1078–1079.
[17] I. A. Grigor'ev, G. I. Shchukin, L. B. Volodarsky, *Russ. Chem. Bull.* **1986**, *35*, 2081–2086.
[18] M. N. Timofeeva, A. B. Ayupov, A. M. Volodin, J. P. Pak, G. G. Volkova, G. V. Echevskii, *Kinet. Catal.* **2005**, *46*, 123–128.
[19] A. V. Shugalii, A. V. Kulikov, M. V. Lichina, V. A. Golubev, V. D. Sen', *J. Inorg. Biochem.* **1998**, *69*, 67–77.
[20] S. Kishioka, T. Ohsaka, K. Tokuda, *Electrochim. Acta* **2003**, *48*, 1589–1594.
[21] V. A. Golubev, V. D. Sen', I. V. Kulyk, A. L. Alexandrov, *Russ. Chem. Bull.* **1975**, *24*, 2119–2126.
[22] V. Malatesta, K. U. Ingold, *J. Am. Chem. Soc.* **1973**, *95*, 6404–6407.
[23] L. B. Volodarsky, I. A. Grigor'ev, S. A. Dikanov, V. A. Reznikov, G. I. Shchukin, *Imidazoline Nitroxyl Radicals*, Nauka, Moscow, **1988**, pp. 202–205 (in Russian).
[24] R. A. Cox, K. Yates, *Can. J. Chem.* **1979**, *57*, 2944–2951.
[25] A. J. Kresge, S. G. Mylonakis, Y. Sato, V. P. Vitullo, *J. Am. Chem. Soc.* **1971**, *93*, 6181–6188.
[26] R. A. Cox, K. Yates, *J. Am. Chem. Soc.* **1978**, *100*, 3861–3867.
[27] V. A. Golubev, T. S. Rudyk, V. D. Sen', A. L. Alexandrov, *Russ. Chem. Bull.* **1976**, *25*, 744–750.
[28] A. Israeli, M. Patt, M. Oron, A. Samuni, R. Kohen, S. Goldstein, *Free Rad. Biol. Med.* **2005**, *38*, 317–324.
[29] J. R. Fish, S. G. Swarts, M. D. Sevilla, T. Malinsky, *J. Phys. Chem.* **1988**, *92*, 3745–3751.
[30] M. N. Hughes, H. G. Nicklin, K. Shrimanker, *J. Chem. Soc. Part A* **1971**, 3485–3487.
[31] M. B. Neiman, S. G. Mairanovskii, B. M. Kovarskaja, E. G. Rozantsev, E. G. Gintsberg, *Russ. Chem. Bull.* **1964**, *13*, 1424–1426.
[32] V. D. Sen', V. A. Golubev, T. M. Kosheleva, *Russ. Chem. Bull.* **1979**, *28*, 1847–1850.
[33] J. Lind, G. Merenyj, *J. Phys. Chem. A* **2006**, *110*, 192–197.
[34] V. A. Golubev, V. D. Sen', E. G. Rozantsev, *Russ. Chem. Bull.* **1974**, *23*, 2676–2679.
[35] V. D. Sen', Ph.D. Thesis, Institute of Organic Chemistry, Russian Academy of Sciences, Moscow, **1977**.